Optimization of smooth bores of idealized wind instruments with respect to basic acoustic features

T. Hélie and G. Gandolfi
IRCAM, 1, place Igor-Stravinsky, 75004 Paris, France
thomas.helie@ircam.fr

In this paper, we consider a class of simplified smooth bores of wind instruments which are composed of a mouthpiece, a cylindrical or conical pipe and a bell. The acoustic model under consideration is based on a standard matrix formalism in the Laplace-Fourier domain for which analytic formula are available. The mouthpiece can be modeled by the begining of the bore, or more simply, by a volume to be connected to the bore. The acoustic transfer functions of the bore are derived from the smooth connection of a few lossy acoustic pipes with constant-flared profiles (governed by a refined curvilinear 1D horn equation) concatenated with a radiation load model, which is consistent with spherical wavefronts. These models have proved to be relevant, based on a comparison with measurements on a trombone bell. Then, the geometric parameters of the complete model are optimized according to a constrained objective function. This function is specially designed in order to optimize acoustic targets. A special care is devoted to the tuning of the first resonances according to an ideal harmonic sequence. Results are presented for some typical cylindrical and conical chambers, corresponding to a few sketched instruments without fingerings, that could correspond to some idealized clarinets, trombones, oboes, saxophones or horns.
This work is part of the ANR project CAGIMA.

1 Outline

This paper is organized as follows. Section 2 gives short recalls about the realistic acoustic model of pipes which is used in this paper and introduces some idealized target input impedances for dissipative quarter wave resonators and half wave resonators. Section 3 presents the method to optimize the shape of the realistic pipes, according to the idealized target impedances, and subjected to constraints on the first harmonically related resonance frequencies. Section 4 gives the results. Section 5 ends with conclusions and perspectives.

2 Acoustic model and idealized target impedances

In this section, we give short recalls about a realistic acoustic model of pipes with bibliographic information. Then, we introduce target impedances as those of dissipative resonators with harmonically related resonance frequencies. Two cases are considered: one idealized quarter wave resonator (for straight pipes) and one idealized half wave resonator (for conical pipes).

2.1 Acoustic model

In this paper, we consider acoustic transfer matrices derived from a one-dimensional acoustic model of axi-symmetric pipes with varying cross-section that includes visco-thermal losses. This model is fully detailed in [1] and is not described here for sake of conciseness. It is based on:

(i) a change of coordinates that rectifies isobar maps, combined with an approximation that assumes that isobars are nearly spherical near the wall of the pipe (see [2]);

(ii) the modelling of visco-thermal losses through an equivalent wall admittance (Cremer's admittance);

(iii) the (C^1-regular) smooth connection of pipes with constant parameters that characterize the losses and the geometry (straight pipes, conical pipes, flared pipes and convex chambers);

(iv) a model that approximates the radiation impedance of a pulsating portion of a sphere (detailed in [3]).

The point (i) restores a horn equation in which the space variable is not the axial abscissa z but the curvilinear abscissa ℓ that measures the length of the profile. The point (ii) refines (i) and leads to the so-called "Webster-Lokshin" equation with curvilinear abscissa. The point (iii) yields transfer matrices which are analytic in the Laplace-Fourier domain and which depend on a few geometric parameters so that they are well adapted to optimization issues. Geometric parameters of each segment n are: the left and right radius (R_{n-1}, R_n), the length (L_n) and the constant $\Upsilon_n = \mathcal{R}''(\ell)/\mathcal{R}(\ell)$ which quantifies the curvature of the shape. According to a benchmark, the point (iv) has be proved to be more accurate than radation models based on planar geometries [4]. Moreover, points (i-iv) has proved to be relevant based on a on measurements on a trombone bell [1].

2.2 Target impedance for straight pipes

A conservative straight pipe which is ideally opened at its end ($Z_{load} = 0$) is an exact quarter wave resonator. Such a pipe of length L is characterized by the input impedance $Z_{in}(s) = Z_c \tanh(\tau s)$ in the Laplace domain ($s \in \mathbb{C}_0^+ = \{s \in \mathbb{C} \ s.t. \ \Re e(s) > 0\}$) where $\tau = L/c_0$. Its poles are given by $s_n = i\,\frac{(2n+1)\pi}{2\tau}$ for $n \in \mathbb{Z}$. They correspond to resonances with an infinite quality factor (poles have a zero real part) for a series of odd harmonics with frequency $f_n = (2n+1)/(4\tau) = (2n+1)\frac{c_0}{4L}$ ($n \geq 0$ for positive frequencies).

In this paper, we consider the same series of frequencies but with a constant damping coefficient $\xi > 0$, that is, choosing the target impedance as

$$Z_{in}^{=}(s) = Z_c \tanh(\tau s + \xi) \ \text{ where } \tau = L/c_0, \qquad (1)$$

(poles are $s_n = -\xi + i\,\frac{(2n+1)\pi}{2\tau}$). This impedance is that of a conservative straight pipe loaded by a purely resistive impedance Z_{load} smaller than Z_c where $\xi = \operatorname{atanh}(Z_{load}/Z_c)$.

Note that, at frequencies f_n, $Z_{in}^{=}$ has a zero phase since $Z_{in}^{=}(2i\pi f_n) = Z_c \tanh\left(\xi + i(n\pi + \pi/2)\right) = Z_c/\tanh(\xi) = Z_c^2/Z_{load}$ is real and positive.

An example of such a template impedance is displayed in figure 1.

2.3 Target impedance for conical pipes

The case of truncated conical pipes is more complex. Consider a conservative conical pipe of length $L = L_1 + L_2$, whose part from the apex to length L_1 is removed, and which is ideally opened at its right end. The poles of the input impedance of such a truncated conical pipe are not associated with harmonically related resonance

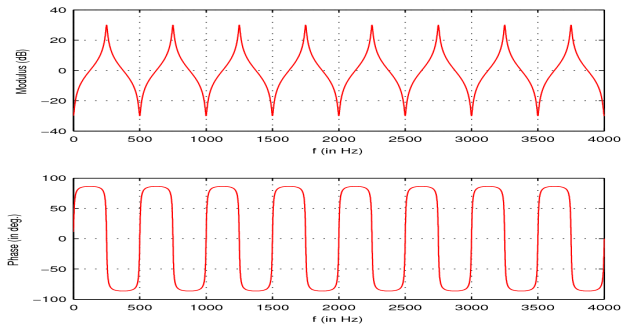

Figure 1: Example of an idealized impedance (1) for a straight pipe (normalized version without Z_c): parameters are chosen such that $f_1 = 250$ Hz for a temperature $T = 20°C$ ($c_0 = 343.4\, m.s^{-1}$ and $L = 343.4\, mm$) and such that $Z^{=}_{in}(2i\pi f_n)$ corresponds to 30 dB ($\xi = 0.0316$).

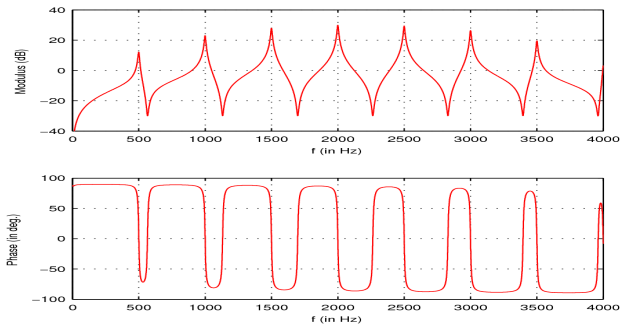

Figure 2: Example of an idealized impedance (2) for a truncated conical pipe (normalized version): the total length is $L = 343.4\, mm$, $\xi = 0.0316$ as in figure 1 ($\xi_1 = 0, \xi_2 = \xi$) and $L_1 = 40$ mm.

frequencies. However, nearly harmonic ones can be recovered by adding a mouthpiece, the volume of which is chosen as that of the missing volume of the cone. In this case, as detailed in [5], the input impedance is close to $Z_{in}(s) = Z_c\Big[\text{cotanh}(\tau_1 s) + \text{cotanh}(\tau_2 s)\Big]^{-1}$, the poles of which are $s_n = i\, n\pi/\tau$ for $n \in \mathbb{Z}$, with $\tau = \tau_1 + \tau_2 = L/c_0$ These poles correspond to the frequencies of an exact half wave resonator ($f_n = n/(2\tau) = nc_0/(2L)$ with $n \geq 1$ for positive ones). In [5], it is specially pointed out that the formula of this impedance is similar to the input admittance of a lossless string of length L, excited at L_1, if only transverse waves are considered.

In this paper, similarly to § 2.2 and (1), we introduce constant damping coefficients $\xi_1, \xi_2 > 0$ and choose the target impedance as

$$Z^{<}_{in}(s) = Z_c\Big[\text{cotanh}(\tau_1 s + \xi_1) + \text{cotanh}(\tau_2 s + \xi_2)\Big]^{-1} \qquad (2)$$

(poles are $s_n = -\xi + i\,\frac{n\pi}{\tau}$ where $\tau = \tau_1 + \tau_2$ and $\xi = \xi_1 + \xi_2$). Choosing $\xi_1 = 0$ and $\xi_2 = \xi > 0$ corresponds to an ideal conservative boundary condition at left and a purely resitive boundary condition at right.

Note that the choice of this template impedance is based on a sequence of poles with a constant damping and harmonically related frequencies f_n. However, the phase of $Z^{<}_{in}$ at these frequencies is not zero in general: for (2), the definition of the resonance frequencies based on a (decreasing) zero phase does not coincide with that based on the imaginary part of poles (that is the eigenfrequencies). In this paper, we consider a small truncated part ($L_1 \ll L_2$) so that a nearly zero phase is recovered: this makes the two concepts of resonance frequency (zero phase versus imaginary part of the poles) nearly coincide. Such a template impedance is displayed in figure 2.

3 Optimization method

In this section, an optimization of the bore geometry is developed, according to an objective function under constraints. This function provides a well-suited distance between a acoustic impedance (a target) and the realistic model described in § 2.1. It can be used to recover the smooth shape of resonators from measured iinput mpedances (see [6]) or, here, to find smooth shapes that are the closest to idealized target impedances.

To establish this tool, a configuration space is first specified: this corresponds to the "space of possibilities" (§ 3.1). Second, a set of relevant objective functions is proposed (§ 3.2), from which a selection will be extracted to build the final algorithm. Then, as the optimization problem is nonlinear and non convex, no exact solver is available: the strategy is to build an algorithm which follows a scenario with increasing requirements (§ 3.3), that provide usable results in practice.

3.1 Parameters and configuration space

The model is composed of concatenated segments ended by an acoutic radiation load. Physical constants are fixed. For each segment, geometrical parameters are:

- Radius R_l and R_r at extremities,
- Length L,
- Quantity Υ ($\Upsilon < 0$ for convex chambers, $\Upsilon = 0$ for straight and conical pipes, $\Upsilon > 0$ for flared pipes).

The geometric parameters used for the radiation load (sphere radius and characteristic angle) are straightforwardly deduced from the geometry of the end segment. Over $4N$ parameters for N segments, smooth junctions (C^1-regularity) fix $2(N-1)$ contraints. Hence, the number of degrees of freedom (DOFs) of the model composed of N segments is

$$4N - 2(N-1) = 2N + 2 \text{ DOFs.} \qquad (3)$$

The free parameters are chosen as follows: radius R_n at each junction and at extremities (N+1), length L_n (N), and the slope at the left extremity of the first segment (1).

Furthermore, these parameters must be consistent with a validity domain due to structural reasons (positive radius, bounded maximal slope $|\mathcal{R}'(\ell)| \leq 1$, which is mapped to a vertical slope for the axial abscissa z), or due to the validity of simplifying assumptions (non capilar pipes, curvature radius of the shape sufficiently large, etc), or even, due to practical reasons (2mm< R to be defined by the instrument maker, segment length sufficiently large, etc). In this work, only bores without convex chambers (straight, conical and flared pipes) are considered so that $\Upsilon \geq 0$. The corresponding configuration space is summarised in table 1.

Parameters	Constraint	DOF
R_n	$\geq R_{min} = 2.10^{-3}$ m	$+2N$
L_n	$\geq L_{min} = 5.10^{-3}$ m	$+N$
Υ_n	≥ 0	$+N$
structural	continuity	$-N+1$
structural	continuous derivative	$-N+1$
structural	abs($\mathcal{R}'$) ≤ 1	0

Table 1: Description of the configuration space for N segments: parameters, constraints and DOFs.

3.2 Objective function

3.2.1 Weighted square error

The proximity between the acoustic target and the model is measured through an objective function based on a weighted quadratic error

$$C(\Theta) = \int_{f_{min}}^{f_{max}} E_\Theta(f) W(f)\, \mathrm{d}f, \tag{4}$$

where $[f_{min}, f_{max}]$ is the frequency range on which a quadratic error $E_\Theta(f)$ between the target and the model (with parameters Θ) is to be minimized, following a local weight $W(f)$ ($W(f) = 1$ for a uniform weight).

Several alternatives can be used: (i) discrepancy between normalized input impedances $Z = (P/V)/(\rho_0 c_0)$ or between the associated reflexion functions $R = (Z-1)/(Z+1)$; (ii) several types of errors (simple or relative errors, or relative error adjusted with respect to the variance of measurement errors (see [6] or some uncertainties). These alternatives are summarized in table 2.

	Quadratic error		
	simple	relative	relative+adjus.
Z_{mod}	$\left\lvert Z_{mod} - Z_{trgt}\right\rvert^2$	$\left\lvert 1 - \frac{Z_{mod}}{Z_{trgt}}\right\rvert^2$	$\left\lvert 1 - \frac{Z_{mod}\overline{Z_{trgt}}}{\lvert Z_{trgt}\rvert^2+\sigma^2}\right\rvert^2$
R_{in}	$\left\lvert R_{mod} - R_{trgt}\right\rvert^2$	$\left\lvert 1 - \frac{R_{mod}}{R_{trgt}}\right\rvert^2$	$\left\lvert 1 - \frac{R_{mod}R_{trgt}}{R_{trgt}+\sigma^2}\right\rvert^2$

Table 2: Quadratic errors E: Z_{mod} and R_{mod} are associated with models, Z_{trgt} and R_{trgt} with targets, and σ^2 denotes the variance of measurement errors or some uncertainties.

3.2.2 Constraints on resonances and anti-resonances

A first crucial point is to represent the frequencies of the first resonances (/anti-resonances) of the target in an exact (a) or accurate (b) way. Here, these frequencies are defined by a null phase of the input impedance (dissipation without reactive term), when decreasing (/increasing).

Two approaches are proposed to reach this objective. The first one (a) consists in adding as many equality contraints as selected exact frequencies to the objective function (4). In the sequel, these constraints of zero crossing phase for the selected peaks are denoted (ZCP). The second approach (b) consists in choosing a well-suited weight function W that emphasize resonances and anti-resonances zones. An example is

$$W(f) = \frac{\mathfrak{R}e\left(X_{trgt}(f)\right)^2}{\left\lvert X_{trgt}(f)\right\rvert^2} = \cos^2\left(\arg\left(X_{trgt}(f)\right)\right) \tag{5}$$

where X_{trgt} can be Z_{trgt} or R_{trgt}.

Note that a third standard approach consists in adding a penalty function to the objective function. This is not investigated here.

3.2.3 Practical facilities

For practical reasons, additional constraints can be added by the user such as bounds on the total length, the maximal radius, geometrical configuration of extremities (radius, slope of the shape). These constraints are denoted (UC) in the sequel.

3.2.4 Summary and remarks

Contraints (ZCP) and (UC) are summarized in table 3. Each frequency alignment and each contraint of (UC) reduce the number of DOF by one unit.

Parameter	Constraint	DOF
K_1 frequencies (resonance/anti)	$\arg\left[Z_{mod}(f_k)\right] = 0$ s.t. $\arg\left[Z_{trgt}(f_k)\right] = 0$	$-K_1$ (adjustable)
R_0, R_0', R_N, etc	fixed or free	(adjust.) $-K_2$

Table 3: Constraints (ZCP) and (CU), summary of DOF.

In practice, for $K = K_1 + K_2$ constraints, the number of DOFs $2N + 2 - K$ must be sufficiently large to allow the optimizer to reach a sufficiently low quadratic error on the frequency range $[f_{min}, f_{max}]$.

3.3 Algorithm

The algorithm is based on a sequence of optimizations of objectives functions with increasing requirements: at each step, the initialization is chosen as the result of the previous step. Contraints due to the configuration space and the user (UC) are considered from step 1. Contraints (ZCP) are introduced at step 2. These optimizations under constraints are performed by using the algorithm SQP [7] (available in Matlab through function `fmincon`).

The algorithm is composed of the following sequence:

Step 0: Choice of a rough initialization,
(typically, a set of simple segments such as straight or conical pipes, the total length of which is adjusted according to the first peak, or a heuristic choice based on tests and comparison)

Step 1: Optimization of the (adjusted) relative quadratic error, applied to the acoustic input impedance Z, under constraints (CS) et (UC) only,

Step 2: Optimization of the same objective function under constraints (CS), (UC) and (ZCP),

Step 3: Idem for the objective function applied to the reflection function R.

In this sequence, the weight function W is considered to be a parameter of the algorithm: it is fixed to the uniform weight ($W = 1$) or to (5).

4 Results

This section presents results obtained for the target impedances given by (1) and (2), for quarter wave and half wave resonators, respectively. The algorithm is tested in the case where no "acoustic volume" is placed before the pipe: here, the mouthpiece is supposed to be included in the profile which is composed of $N = 5$ segments.

4.1 Quarter wave resonator

We consider the target impedance presented in § 2.2 and figure 1. The initialization corresponds to $R_0 = 7.4\,mm$, $L = 343.4\,mm$ and the profile displayed in figure 3. The associated (normalized) impedance is displayed in figure 3.

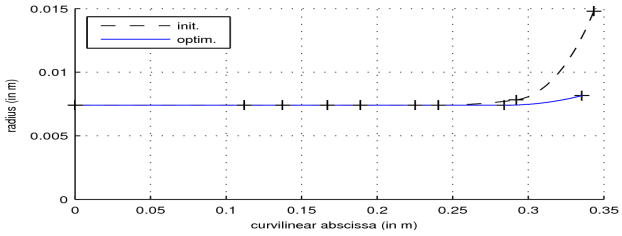

Figure 3: Quarter wave resonator (Step 1): initial profile and result of the algorithm at step 1.

The optimization algorithm is performed with a uniform weight ($W = 1$) and for the frequency range $[1, 4000]$ (in Hz). The constraint (UC) is limited to $R_0 = 7.4$ mm. The first step of the algorithm (no constraint on the phase) provide the profile and the impedance given in figures 3 and 4.

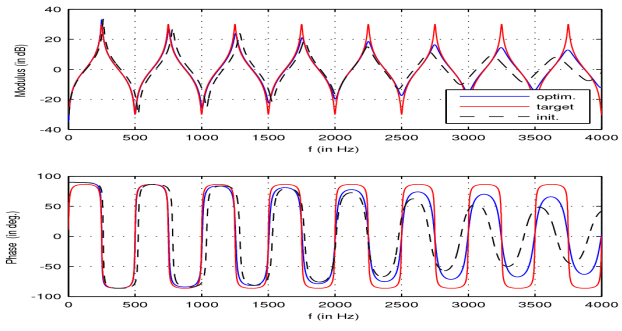

Figure 4: Quarter wave resonator (Step 1): input impedance of the target and for the initial profile and the optimization at step 1.

The second and third steps are performed for 5 constraints (ZCP) on the five first zero-crossing phases (decreasing and increasing). The optimization algorithm (fmincon) fails to guarantee the constraints (ZCP) if all parameters Υ_n are positive, meaning that convex chambers are required. The final results are displayed in figure 5 for the profile, figure 6 for the input impedance, and figure 7 for the input reflection function.

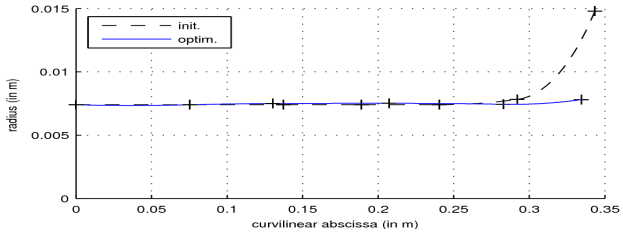

Figure 5: Quarter wave resonator (Step 3): initial profile and result of the algorithm at step 3.

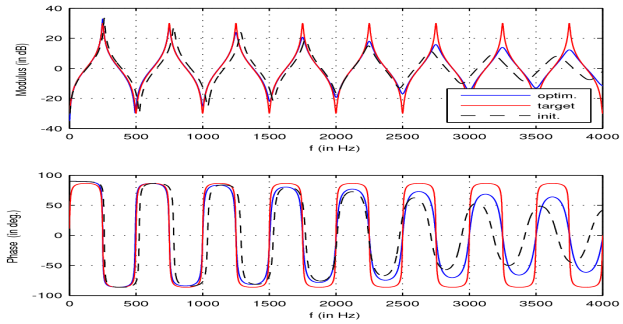

Figure 6: Quarter wave resonator (Step 3): input impedance of the target and for the initial profile and the optimization at step 3.

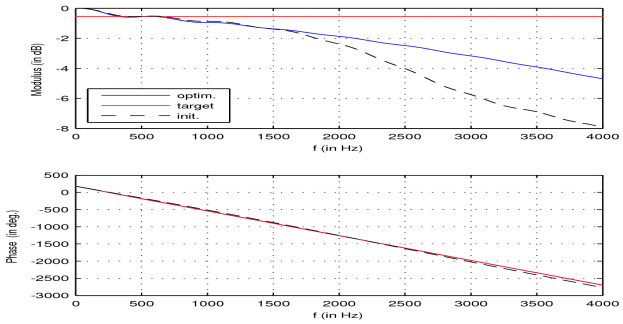

Figure 7: Quarter wave resonator (Step 3): input impedance of the target and for the initial profile and the optimization at step 3.

Note that the bell (typically of a clarinet) is weakened. This is expected and due to the constant and high quality factor of the resonances of the target impedance. This makes the radiated power quite low. In order to increase this power, the target could be modified. But another interesting way is proposed in the perspectives.

4.2 Conical pipe

We consider the target impedance presented in § 2.3 and figure 2. The initialization corresponds to $R_0 = 2\,mm$, length $L_2 = L_{tot} - L_1 = 343.4 - 40 = 303.4\,mm$, and the profile displayed in figure 8. The corresponding impedance is displayed in figure 8. The algorithm is performed in the same conditions as in § 4.1 and with $R_0 = 2$ mm for the

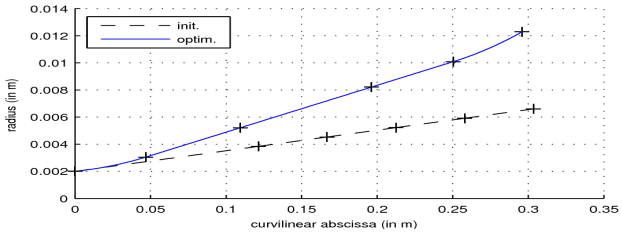

Figure 8: Quarter wave resonator (Step 1): initial profile and result of the algorithm at step 1.

constraint (UC). All the constraints are achieved and the final results are displayed in figure 9 for the profile, figure 10 for the input impedance, and figure 11 for the input reflection function.

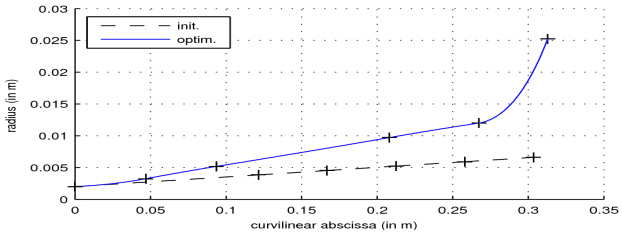

Figure 9: Quarter wave resonator (Step 3): initial profile and result of the algorithm at step 3.

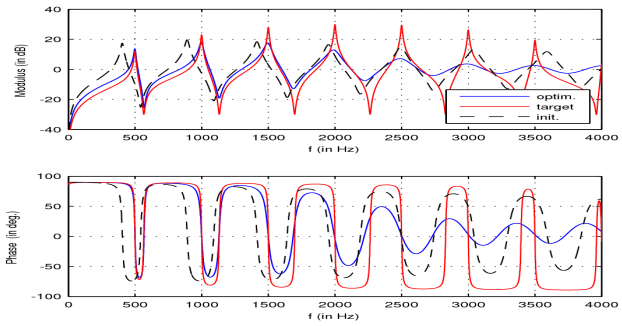

Figure 10: Quarter wave resonator (Step 3): input impedance of the target and for the initial profile and the optimization at step 3.

Contrarily to the quarter wave resonator, the constraint (CPZ) emphasizes the bell, at the end of a quasi-conical pipe. However, the final radius is large (about 25cm). In order to obtain a more practicable profile, an upper bound on the radius in the constraint (UC) has still to be included in a future work.

5 Conclusion and perspectives

In this paper, a method to improve the harmonicity of straight and conical acoutic pipes has been presented. This method is based on the optimization of a realistic lossy acoustic model of axi-symmetric pipes with smooth shapes, according to a specially designed objective function and constraints. The first practical results show that quarter wave resonators can be related to nearly straight pipes. But, to reach harmonically related resonances frequencies, they must include convex chambers. For half wave resonators,

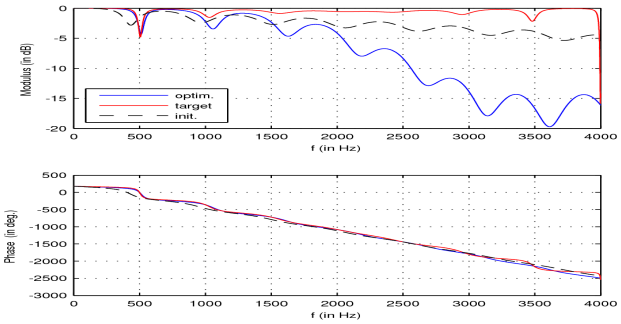

Figure 11: Quarter wave resonator (Step 3): input impedance of the target and for the initial profile and the optimization at step 3.

the results make appear a change of conicity at the begining of the pipe combined with an “emphasized bell”.

In order to go towards the design of musical instruments in practice, several improvements are concerned with:

- including a maximal radius;
- increasing the number of segments (and so the DOFs) to refine the results and increase the number of contraints on the resonance frequencies;
- including holes and their effect on the input impedance and their external radiation to handle real instruments;
- minimizing of a distance between input impedances (or input reflexion functions) on a frequency range $[f_1, f_2]$ and maximizing the radiated power beyond f_2.

Acknowledgments

The authors thanks Jean-Pierre Dalmont for having transmitted interesting bibliographic information. This work is part of the project CAGIMA supported by the French Research National Agency.

References

[1] T. Hélie, T. Hézard, R. Mignot, and D. Matignon. One-dimensional acoustic models of horns and comparison with measurements. *Acta acustica united with Acustica*, 99-6:160–174, 2013.

[2] T. Hélie. Mono-dimensional models of the acoustic propagation in axisymmetric waveguides. *J. Acoust. Soc. Amer.*, 114:2633–2647, 2003.

[3] T. Hélie and X. Rodet. Radiation of a pulsating portion of a sphere: application to horn radiation. *Acta Acustica united with Acustica*, 89:565–577, 2003.

[4] P. Eveno, J.-P. Dalmont, R. Caussé, and J. Gilbert. Wave propagation and radiation in a horn: Comparisons between models and measurements. *Acta Acustica*, 98:158–165, 2012.

[5] S. Ollivier, J.P. Dalmont, and J. Kergomard. Idealized models of reed woodwinds. Part I : analogy with the bowed string. *Acta Acustica united with Acustica*, 90(6):1192–1203, 2004.

[6] T. Hélie, G. Gandolfi, and T. Hézard. Estimation paramétrique de la géométrie de la perce d’un instrument ŕ vent ŕ partir de la mesure de son impédance acoustique d’entrée. In *Congrčs Français d’Acoustique*, volume 12, pages 1–7, Poitiers, France, 2014.

[7] J. Nocedal and S. Wright. *Numerical Optimization*. Springer, 1999.